Electrochemical investigation of uncapped $AgBiS_2$ (Schapbachite) synthesized by *in situ* melts of xanthate precursors

Malik Dilshad Khan,[a]* Muhammad Aamir,[b] Manzar Sohail,[c] Sanket Bhoyate,[d] Megan Hyatt,[e] Ram K. Gupta,[d] Muhammad Sher,[f] Neerish Revaprasadu,[a]*

[a]Department of Chemistry, University of Zululand, Private Bag X1001, Kwa-Dlangezwa, 3880, South Africa.

[b]Materials Lab, Department of Chemistry, Mirpur University of Science and Technology, Allama Iqbal Road, Mirpur AJK, Pakistan.

[c]Centre of Research Excellence in Nanotechnology, King Fahd University of Petroleum and Minerals, Dhahran, 31261, Saudi Arabia.

[d]Department of Chemistry, Pittsburg State University, Pittsburg, KS 66762, USA.
[e]Labette County High School, Altamont, KS 67330, USA.
[f]Department of Chemistry, Allama Iqbal Open University, Islamabad, Pakistan.

*E-mail: RevaprasaduN@unizulu.ac.za

Supplementary Data

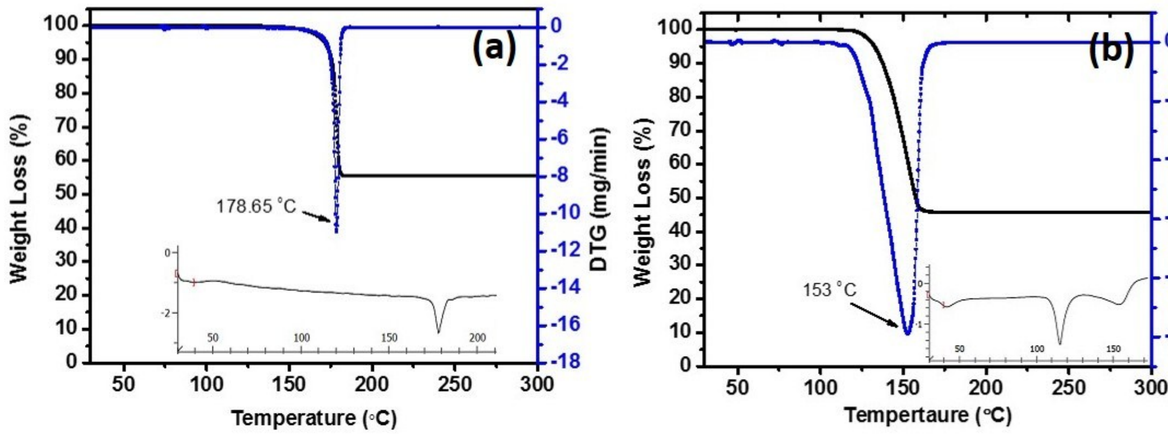

Figure S1. TGA and heat flow curves for (a) (*O*-ethyldithiocarbonato)silver(I) and (b) *tris*(*O*-ethyldithiocarbonato)bismuth(III) complex.

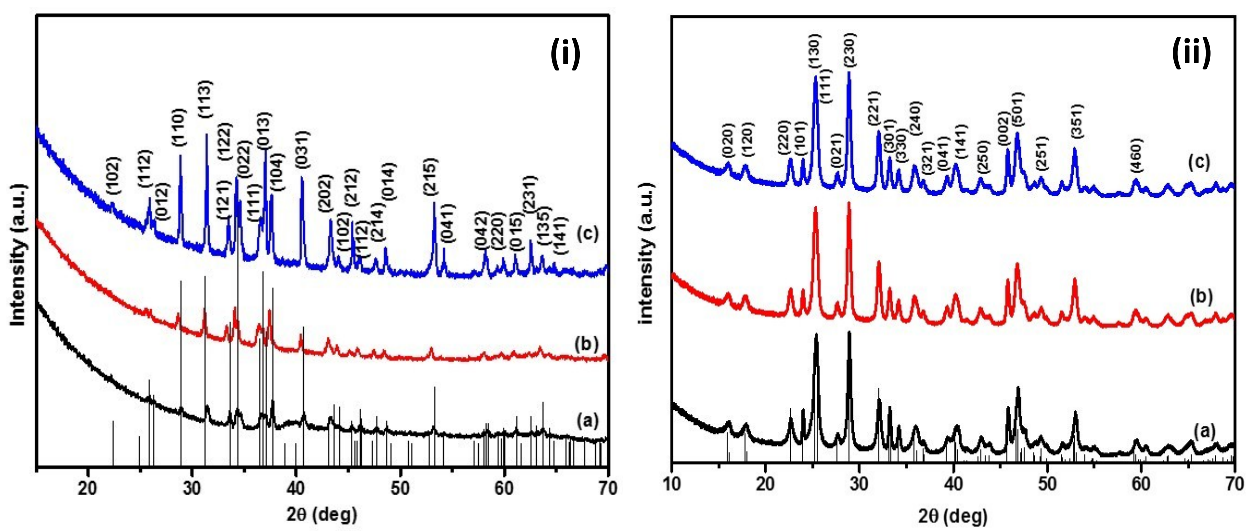

Figure S2 (i) p-XRD pattern of monoclinic Ag_2S (acanthite, ICDD # 00-024-0715) synthesized by pyrolysis of (*O*-ethyldithiocarbonato)silver(I) complex at (a) 200 °C, (b) 250 °C and (c) 300 °C. (ii) p-XRD pattern of orthorhombic Bi_2S_3 (bismuthinite, ICDD# 01-075-1306) synthesized by pyrolysis of *tris*(*O*-ethyldithiocarbonato)bismuth(III) complex at (a) 200 °C, (b) 250 °C and (c) 300 °C.

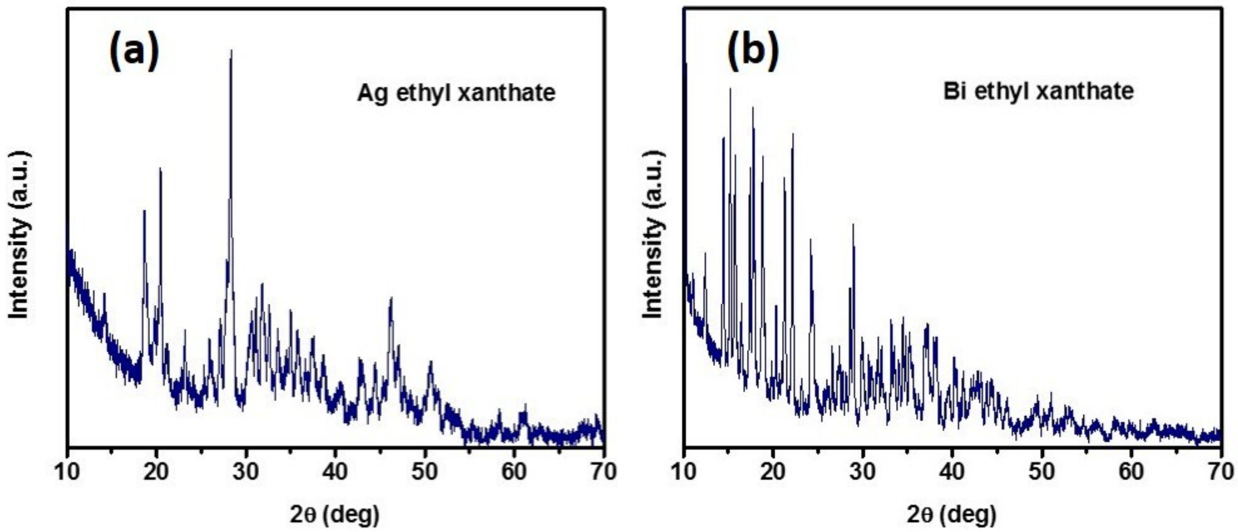

Figure S3. p-XRD of (a) silver ethyl xanthate and (b) bismuth ethyl xanthate, complexes.

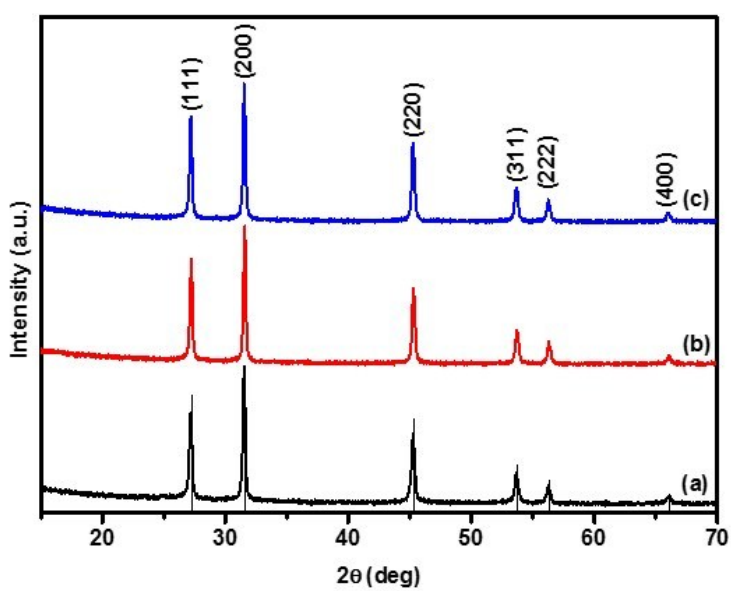

Figure S4. p-XRD pattern of cubic $AgBiS_2$ (schapbachite) synthesized at (a) 200 °C, (b) 250 °C and (c) 300 °C by melt method.

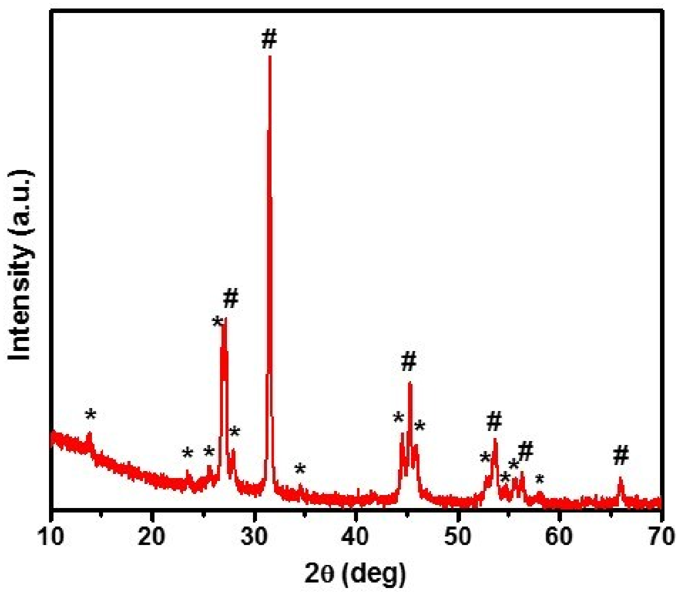

Figure S5. p-XRD pattern of $AgBiS_2$ synthesized at 150 °C, where (*) represent the peaks for matildite phase and (#) represent schapbachite phase.

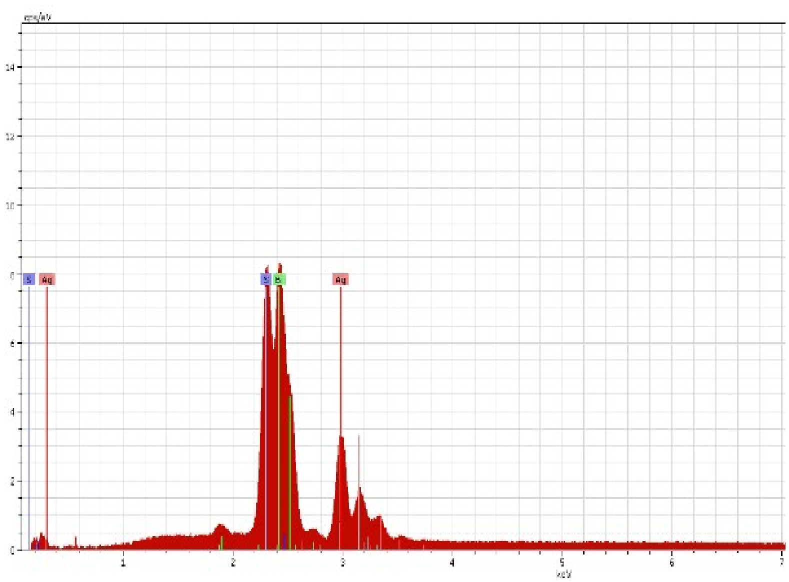

Figure S6. EDX spectrum of $AgBiS_2$ synthesized at 250 °C.

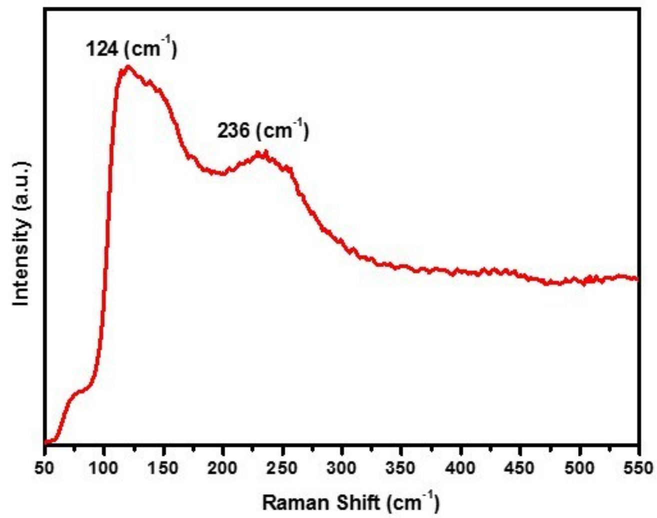

Figure S7. Raman spectrum of $AgBiS_2$ synthesized at 250 °C.

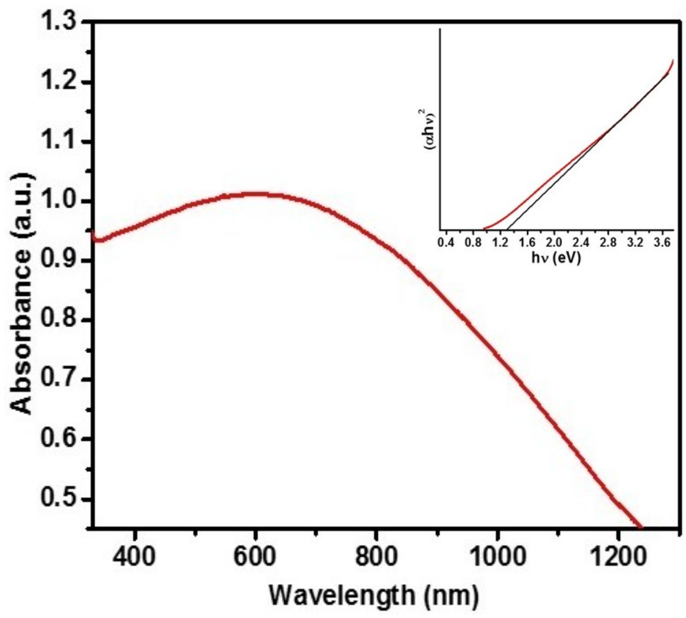

Figure S8. UV-Vis-NIR spectrum of $AgBiS_2$ and (inset) shows estimated band gap by Tauc plot.

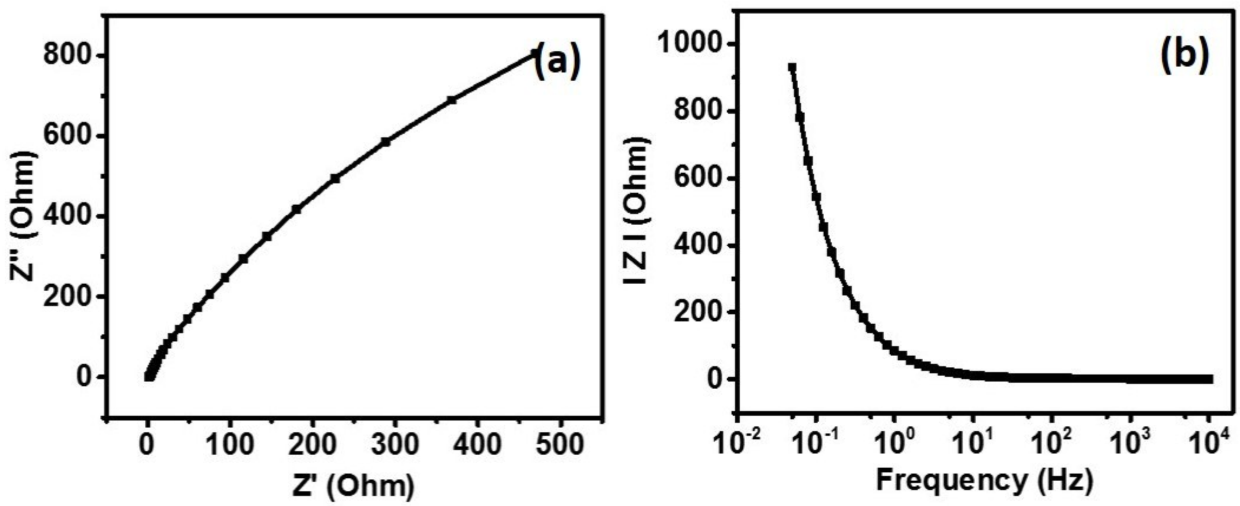

Figure S9. (a) Zreal vs. Zimg plot and (b) |Z| vs. frequency plot for $AgBiS_2$.

Table S1. Comparison of specific capacitance of other reported oxide and sulfide-based materials.

Samples	**Specific capacitance (F/g)**	**Reference**
Bi_2S_3-Graphene composite	290	[1]
Microwave-assisted CoS	224	[2]
CoS	~435	[3]
$CuCo_2O_4$	809	[4]
$CuCo_2S_4$	443	[5]
$NiCo_2O_4$ films on ITO	490	[6]
$NiCo_2O_4$ coral-like porous crystals	217	[7]
$NiCo_2S_4$	800	[8]
$NiCo_2S_4/Fe_2O_3$	342	[9]
$AgBiS_2$	440	**This work**

1. Vadivel, S.; Naveen, A. N.; Kamalakannan, V.; Cao, P.; Balasubramanian, N., Facile large scale synthesis of Bi2S3 nano rods–graphene composite for photocatalytic photoelectrochemical and supercapacitor application. *Applied Surface Science* **2015,** 351, 635-645.
2. You, B.; Jiang, N.; Sheng, M.; Sun, Y., Microwave vs. solvothermal synthesis of hollow cobalt sulfide nanoprisms for electrocatalytic hydrogen evolution and supercapacitors. *Chemical Communications* **2015,** 51, (20), 4252-4255.
3. Meng, X.; Deng, J.; Zhu, J.; Bi, H.; Kan, E.; Wang, X., Cobalt sulfide/graphene composite hydrogel as electrode for high-performance pseudocapacitors. *Scientific reports* **2016,** 6, 21717.
4. Vijayakumar, S.; Lee, S.-H.; Ryu, K.-S., Hierarchical CuCo2O4 nanobelts as a supercapacitor electrode with high areal and specific capacitance. *Electrochimica Acta* **2015,** 182, 979-986.
5. Xu, Y.; Zhou, T.; Cao, X.; Zhao, W.; Chang, J.; Zhu, W.; Guo, W.; Du, W., Low-cost synthesis and electrochemical characteristics of ternary Cu-Co sulfides for high performance full-cell asymmetric supercapacitors. *Materials Research Bulletin* **2017,** 91, 68-76.
6. Salunkhe, R. R.; Jang, K.; Yu, H.; Yu, S.; Ganesh, T.; Han, S.-H.; Ahn, H., Chemical synthesis and electrochemical analysis of nickel cobaltite nanostructures for supercapacitor applications. *Journal of Alloys and Compounds* **2011,** 509, (23), 6677-6682.
7. Wu, Y. Q.; Chen, X. Y.; Ji, P. T.; Zhou, Q. Q., Sol–gel approach for controllable synthesis and electrochemical properties of NiCo2O4 crystals as electrode materials for application in supercapacitors. *Electrochimica Acta* **2011,** 56, (22), 7517-7522.
8. Xiao, T.; Li, J.; Zhuang, X.; Zhang, W.; Wang, S.; Chen, X.; Xiang, P.; Jiang, L.; Tan, X., Wide potential window and high specific capacitance triggered via rough NiCo2S4 nanorod arrays with open top for symmetric supercapacitors. *Electrochimica Acta* **2018,** 269, 397-404.
9. Jia, R.; Zhu, F.; Sun, S.; Zhai, T.; Xia, H., Dual support ensuring high-energy supercapacitors via high-performance NiCo2S4@ Fe2O3 anode and working potential enlarged MnO2 cathode. *Journal of Power Sources* **2017,** 341, 427-434.